Journal of Marine Science and Technology

Volume 20 | Issue 5 Article 2

AN EXCITED SYSTEM DESIGN FOR THE MAXIMUM OUTPUT OF INDUCTION GENERATOR BASED ON VECTOR CONTROL

Ding-Tsair Su
Department of Electrical Engineering, Chienkuo Technology University, Changhua, Taiwan, R.O.C.

Ying-Shing Shiao
Department of Electrical Engineering, National Changhua University of Education, Changhua, Taiwan, R.O.C.

Koan-Yuh Chang
Department of Electrical Engineering, Chienkuo Technology University, Changhua, Taiwan, R.O.C.

Wen-Jer Chang
Department of Marine Engineering, National Taiwan Ocean University, Keelung, Taiwan, R.O.C.,
wjchang@mail.ntou.edu.tw

Follow this and additional works at: https://jmstt.ntou.edu.tw/journal

 Part of the Engineering Commons

Recommended Citation

Su, Ding-Tsair; Shiao, Ying-Shing; Chang, Koan-Yuh; and Chang, Wen-Jer (2012) "AN EXCITED SYSTEM DESIGN FOR THE MAXIMUM OUTPUT OF INDUCTION GENERATOR BASED ON VECTOR CONTROL," *Journal of Marine Science and Technology*: Vol. 20: Iss. 5, Article 2.
DOI: 10.6119/JMST-011-0318-3
Available at: https://jmstt.ntou.edu.tw/journal/vol20/iss5/2

This Research Article is brought to you for free and open access by Journal of Marine Science and Technology. It has been accepted for inclusion in Journal of Marine Science and Technology by an authorized editor of Journal of Marine Science and Technology.

Journal of Marine Science and Technology, Vol. 20, No. 5, pp. 485-491 (2012)
DOI: 10.6119/JMST-011-0318-3

AN EXCITED SYSTEM DESIGN FOR THE MAXIMUM OUTPUT OF INDUCTION GENERATOR BASED ON VECTOR CONTROL

Ding-Tsair Su[1], Ying-Shing Shiao[2], Koan-Yuh Chang[1], and Wen-Jer Chang[3]

Key words: vector control, inverter, induction generator, VSCF system, *dq* axes theory, digital signal processor.

ABSTRACT

In this paper, without using the mechanical speed regulator, we propose a scheme that can control the output power of an induction generator by controlling the excited current. To attain this goal, an inverter is designed as a current controlled source, to supply an excited current for the induction generator. Furthermore, using the *dq* axes theory, a vector controller is designed by a digital signal processor (DSP) for controlling the inverter which supplies excited current appropriately in accordance with the wind speed to regulate the induction generator output power. Finally, the experimental results have shown good performances of the proposed inverter for control the excited current on induction generator. Thus, in applications of wind power generation, the proposed system can successfully obtain the variable speed constant frequency (VSCF) control without using the mechanical speed regulator in wind power applications.

I. INTRODUCTION

Owing to the merits of brushless, excited source useless, simple and rigid structure, simple operation, easy maintenance and etc., the induction generator has been used widely in the generation of wind power. However, the induction generator with a squirrel cage rotor lacks a self-excited source and consequently can not generate the reactive power needed for power generating. Therefore, an induction generator for independent operating must have a capacitor connected in parallel to the output terminal so as to provide the reactive power and use the capacitor exciter. Since the variation of wind speed affects the operation speed of wind power generator, and then it will influence the rotation speed of the rotor for induction generator to be driven. This phenomenon will lead to the variation of output voltage and frequency accordingly, such that the normal rated power can not be outputted and the utilizing of induction generator is lowered [17, 18].

Many papers have been written to improve the above drawbacks. Some approaches use thyristor for controlling the voltage on the load end with closed-loop form. However, considering the problems of the cost invested on the system is high and the controlling circuit is complicated, harmonics of high order and surge for thyristor switching turn on and turn off are difficult to solve, these approaches have the drawbacks of low system reliability and bad system stability [10]. Studtmann brought up the research on using a pulse-width-modulation (PWM) inverter as the controller of a self-excited induction generator, in which the PWM inverter plays the role of an adjustable capacitor and can be adapted to the induction generator and the reactance of load [15]. Afterward, using the rectifier and the inverter, the objective of research is to combine two-stage AC-DC-AC inverter with the self-excited induction generator to modulate the alternating power source of variable frequency into that of constant frequency as the utilization of load [8]. Therefore, the problem that the value of output power varies with the rotating speed and the load of a self-excited induction generator can be effectively solved [12, 13].

In early periods, the non-linear relations and mathematic modes of an induction machine are too complicated to handle the dynamic characteristic and thus the development of induction machine in applications of variable speed is obstructed. In 1972, Blaschke from Siemens in Germany proposed a vector control theory and start a new generation for alternating current motors [1]. Its basic concept is to change the complicated state equation of an induction machine into a non-time-variable and non-coupling mathematic model by using the *dq* axes theory and technique of frame transformation, so that the armature current and the magnetic field current can be controlled separately. This control method is easy and likes as a shunt DC motor which the output torque can be controlled by

Paper submitted 03/16/09; revised 06/15/10; accepted 03/18/11. Author for correspondence: Wen-Jer Chang (e-mail: wjchang@mail.ntou.edu.tw)
[1] *Department of Electrical Engineering, Chienkuo Technology University, Changhua, Taiwan, R.O.C.*
[2] *Department of Electrical Engineering, National Changhua University of Education, Changhua, Taiwan, R.O.C.*
[3] *Department of Marine Engineering, National Taiwan Ocean University, Keelung, Taiwan, R.O.C.*

just controlling the armature current.

According to methods of obtaining magnetic field angles for alternating generator, the magnetic field vector controls can be divided into the direct and indirect control methods. The former calculates the value and position of magnetic flux with estimating rules by measuring the electrical parameters such as the current and voltage of the motor, while the latter first adds the slip angular frequency by estimating to the electrical rotating speed of motor shaft by measuring, here the sum of these two values is called the angular frequency of magnetic flux, then the angular angle of magnetic flux can be obtained by integrating the angular frequency of magnetic flux. Furthermore, according to the classification of reference frames of magnetic flux, the magnetic field vector controls can be divided into the stator-flux-oriented control, the rotor-flux-oriented control and the airgap-flux-oriented control. In which, with respect to the complexity of equation for induction generator magnetic field orientation control, the rotor-flux-oriented control is the most simple control method [5, 11, 14].

However, in practical application, the vector control needs complicated mathematical calculations and could not be achieved by the analogical circuit, thus it is not used for a period of time. Now the complicated control rules can be implemented by software based on micro-processor, especially the development of digital signal processor, and then the requirement of high-performance control system can be achieved [3, 9, 16]. In this paper, based on DSP as the core of system control, the vector control of inverter for induction generator is designed. And, with respect to the VSCF system, a vector control is also proposed by combining flux control and decoupling current control of the induction generator. From experiments and computer simulations, it is shown that an inverter can work as the exciting source of an induction generator and the proposed system can successfully obtain the control of VSCF without using the mechanical speed regulator.

II. CONTROL METHOD OF INDUCTION GENERATOR

1. Vector Control

Transform the three phase voltage V_a, V_b and V_c along with the three phase's current i_{aM}, i_{bM} and i_{cM} of the induction machine into the *dq* axes rotating synchronously, then the induction machine will have characteristics similar to that of a DC generator [12, 16]. As shown in Fig. 1, the magnetic field component current i_{dsM} is a vector orthogonal to the vector of torque component current i_{qsM}. Here, the i_{dsM} and i_{qsM} are resemble respectively to the magnetic field current and the armature current of the DC generator. When the rotating speed is raised from sub-synchronous to above synchronous, the magnetic field component i_{dsM} is unchanged but the armature current component is changed from motor mode $+i_{qsM}$ to generator mode $-i_{qsM}$.

The vector control of induction machine is generally used in the motor mode, controlling the magnetic field component

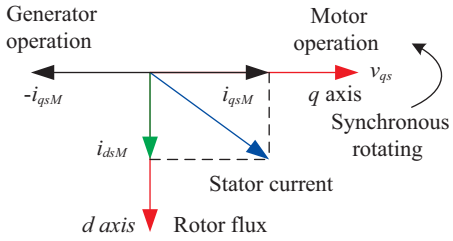

Fig. 1. Vector control of induction machine.

i_{dsM} and the torque component current i_{qsM} to satisfy the torque-speed characteristic of load, and then the control of rotating speed is achieved [4, 6]. In this paper, the vector control is applied in the generator mode of the induction machine; the inverter is controlled to provide the exciting current i_{dsM} needed for the induction machine. Also, the synchronous rotating magnetic field is build, the primary machine drives the induction machine to rotate above synchronous, and the inverter is controlled to modulate the output current $-i_{qsM}$ of the induction generator.

The control signal i^*_{dsI} of the inverter controls the inverter to provide the excited current so as to build the rotating magnetic field of the induction machine and provide the reactive power current needed for the load. Another control signal i^*_{qsI} of the inverter controls the real power current between the induction machine and the load, the control rules are shown as following equations:

$$i^*_{dsI} = i_{dsM} + i_{dL} \tag{1}$$

$$i^*_{qsI} = i_{qsM} + i_{qL} \tag{2}$$

where the i_{dsM} and i_{qsM} are the stator current component, respectively. The i_{dL} and i_{qL} are the load current component, respectively.

2. The Magnetic Flux Control

According to the rotating speed, the vector control of VSCF system for induction generator controls the exciting current i_{dsM} to stabilize the system voltage and then to balance the value of electricity generated and the load demanded. Therefore, the stator current, which is easy controlled, and the rotor magnetic flux are taken as the state variables [7, 16]. After being transformed via three phase *abc* axes to synchronously rotating *dq* axes, the state equation of the induction generator can be expressed as following:

$$p\begin{bmatrix} i_{dsM} \\ i_{qsM} \\ \Phi_{dr} \\ \Phi_{qr} \end{bmatrix} = \begin{bmatrix} -\frac{R_s}{\sigma L_s} - \frac{R_r(1-\sigma)}{\sigma L_r} & \omega & \frac{MR_r}{\sigma L_s L_r^2} & \frac{\omega_r M}{\sigma L_s L_r} \\ -\omega & -\frac{R_s}{\sigma L_s} - \frac{R_r(1-\sigma)}{\sigma L_r} & -\frac{\omega_r M}{\sigma L_s L_r} & \frac{MR_r}{\sigma L_s L_r} \\ \frac{MR_r}{L_r} & 0 & -\frac{R_r}{L_r} & \omega - \omega_r \\ 0 & \frac{MR_r}{L_r} & -(\omega - \omega_r) & -\frac{R_r}{L_r} \end{bmatrix} \begin{bmatrix} i_{dsM} \\ i_{qsM} \\ \Phi_{dr} \\ \Phi_{qr} \end{bmatrix} + \frac{1}{\sigma L_s} \begin{bmatrix} v_d \\ v_q \\ 0 \\ 0 \end{bmatrix} \tag{3}$$

where the Φ_{dr} and Φ_{qr} are the rotor magnetic flux component of synchronously rotating dq axes in induction generator, L_r is the rotor inductance, L_s is the stator inductance, R_r is the rotor resistance, R_s is the stator resistance, M is the mutual inductance between the stator windings, p is the differential operator, ω is the induction generator stator angular frequency (rad/sec), ω_r is the rotor speed of induction generator and $\sigma = 1 - M^2/L_sL_r$ is the coefficient of leakage flux.

The principle of vector control in induction generator is to make Φ_{qr} zero, and to control Φ_{dr}, which is changed inversely to the rotating speed, for stabilizing the system voltage. There by, the magnetic flux component in Eq. (3) can be isolated to following Eq. (4):

$$p\begin{bmatrix}\Phi_{dr}\\ \Phi_{qr}\end{bmatrix}=\begin{bmatrix}-\frac{R_r}{L_r} & \omega-\omega_r\\ -(\omega-\omega_r) & -\frac{R_r}{L_r}\end{bmatrix}\begin{bmatrix}\Phi_{dr}\\ \Phi_{qr}\end{bmatrix}+\frac{MR_r}{L_r}\begin{bmatrix}i_{dsM}\\ i_{qsM}\end{bmatrix} \quad (4)$$

In Eq. (4), let Φ_{qr} to be zero and Φ_{dr} is the controlled quantity, then $p\Phi_{qr} = 0$. If rotating speed of generator is constant for a certain period of time, then Φ_{dr} must also be controlled to a constant value, that is, $\Phi_{dr} = \Psi_{dr}$ and $p\Phi_{dr} = 0$ will be derived. Under this condition, the rotor magnetic flux Ψ_{dr} and the rotor angular frequency ω_{sl} can be obtained by Eq. (4):

$$\omega_{sl} = \omega - \omega_r = \frac{MR_r}{L_r}\frac{i_{qsM}}{\Psi_{dr}} \quad (5)$$

$$p\Psi_{dr} = -\frac{R_r}{L_r}\Psi_{dr} + \frac{MR_r}{L_r}i_{dsM} \quad (6)$$

From Eqs. (5) and (6), as long as the currents i_{dsM} and i_{qsM} are detected, the Ψ_{dr} and ω_{sl} will be obtained. In Fig. 2(a), the difference of the system frequency ω^* and the induction generator rotor speed is the slip angular frequency ω^*_{sl}. The feedback signal i_{dsM} is processed from Eq. (6) and then Ψ_{dr} is obtained. Also, the Ψ_{dr} and i_{qsM} are processed from Eq. (5) to obtain ω_{sl}. Comparing the values of ω_{sl} and ω^*_{sl}, if ω^*_{sl} is larger than ω_{sl} then it means that magnetic flux is insufficient and the exciting current i^*_{dsM} needs to be increased, if on the contrary i^*_{dsM} needs to be decreased. Consequently, processing the error signal of ω_{sl} and ω^*_{sl} via proportional integrator will get the value of magnetic flux Φ^*_{dr}, and this value continue to compared with Ψ_{dr} from Eq. (6) to obtain the error value of magnetic flux, thereby the value of exciting current i^*_{dsM} can be obtained via the magnetic flux controller. Here, in Fig. 2(a), we should point out that the magnetic flux controller is a proportion integrator with limited range.

If the load is only resistance, then the i^*_{dsM} shown in Figs. (2a) and (2b) is the value of the exciting current i_{dsM} provided by the inverter to the induction generator. If the load needs reactive power, the inverter must provide it. Thus, according to Eq. (1), i^*_{dsM} in Fig. 2(b) should plus the reactive power

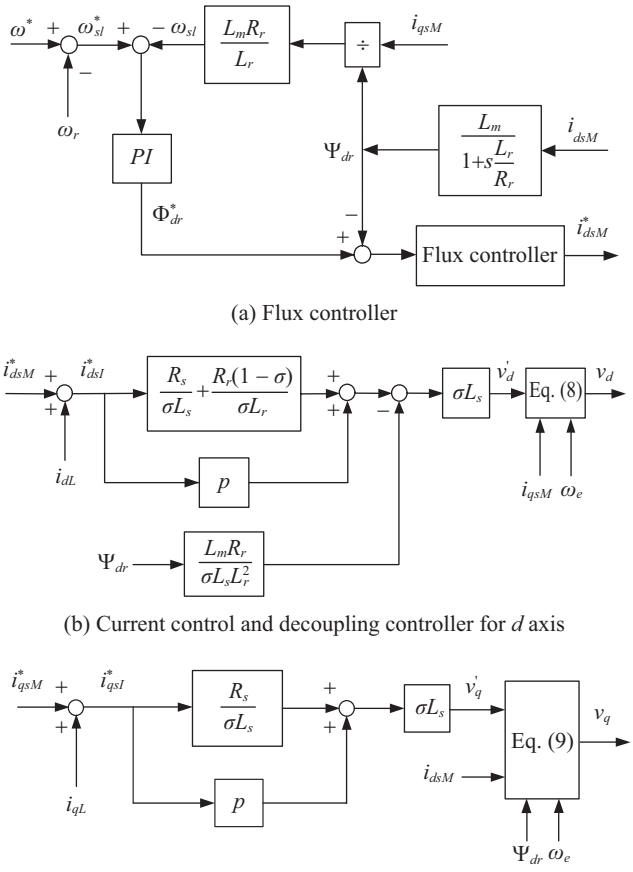

Fig. 2. The vector control of VSCF system for induction generator.

current component i_{dL} of the load and then will be equal to i^*_{dsI} on the inverter. According to Eq. (2), the resistance current component i_{qL} of the load equals to the output current of the induction generator $-i_{qsM}$, then the inverter does not have to provide the q axis current component to the load, that is, the value of i^*_{qsI} on inverter is zero.

If substituting i_{dsM} and i_{qsM} with i^*_{dsI} and i^*_{qsI} in Eq. (3) directly to design the control quantity v_d and v_q, the design value of v_d and v_q will be very difficult because that dq axes are coupling together. Thus, following statement will illustrate how to decouple the dq axes and design the values of v_d and v_q.

3. Decoupling of Current Control

The control principles of the VSCF system of the induction generator are $\Phi_{dr} = \Psi_{dr}$ and $\Psi_{qr} = 0$. With satisfactions of these two conditions, the Eq. (3) can be simplified to Eq. (7).

$$p\begin{bmatrix}i_{dsM}\\ i_{qsM}\\ \Psi_{dr}\end{bmatrix}=\begin{bmatrix}-\frac{R_s}{\sigma L_s}-\frac{R_r(1-\sigma)}{\sigma L_r} & \omega & \frac{MR_r}{\sigma L_sL_r^2}\\ -\omega & -\frac{R_s}{\sigma L_s}-\frac{R_r(1-\sigma)}{\sigma L_r} & -\frac{\omega_r M}{\sigma L_sL_r}\\ \frac{MR_r}{L_r} & 0 & -\frac{R_r}{L_r}\end{bmatrix}\begin{bmatrix}i_{dsM}\\ i_{qsM}\\ \Psi_{dr}\end{bmatrix}+\frac{1}{\sigma L_s}\begin{bmatrix}v_d\\ v_q\\ 0\end{bmatrix} \quad (7)$$

In Eq. (7), d axis and q axis are coupled together, thus the control design becomes difficult. If d axis and q axis can be decoupled, then solution can be simplified as i_{dsM} for controlling v_d and i_{qsM} for controlling v_q. Therefore the following arrangement is done.

$$v_d = v_d' - \omega\sigma L_s i_{qsM} \tag{8}$$

$$v_q = v_q' + \omega[\sigma L_s i_{dsM} + \frac{M}{L_r}\Psi_{dr}] \tag{9}$$

Substituting Eqs. (8) and (9) into Eq. (7), the Eq. (10) can be derived as following:

$$p\begin{bmatrix} i_{dsM} \\ i_{qsM} \\ \Psi_{dr} \end{bmatrix} = \begin{bmatrix} -\frac{R_s}{\sigma L_s} - \frac{R_r(1-\sigma)}{\sigma L_r} & 0 & \frac{MR_r}{\sigma L_s L_r} \\ 0 & -\frac{R_s}{\sigma L_s} & 0 \\ \frac{MR_r}{L_r} & 0 & -\frac{R_r}{L_r} \end{bmatrix} \begin{bmatrix} i_{dsM} \\ i_{qsM} \\ \Psi_{dr} \end{bmatrix} + \frac{1}{\sigma L_s}\begin{bmatrix} v_d' \\ v_q' \\ 0 \end{bmatrix} \tag{10}$$

The approach to realize Eqs. (8)-(10) is shown in Figs. 2(b) and 2(c). In Eq. (10), i_{dsM} and v_d' are separated from i_{qsM} and v_q', thus the current controllers of d axis and q axis can be designed separately.

In Fig. 2(a), the error between of Φ_{dr}^* and Ψ_{dr} generates a control signal i_{dsM}^* via way of flux controller. In Fig. 2(b), the d axis control signal i_{dsI}^* of the inverter is produced by pulsing i_{dsM}^* with i_{dL}. The signal i_{dsI}^* includes i_{dsM}^*, where the d axis control signal v_d' can be designed according to the relationship of i_{dsM} and v_d' in Eq. (10), and becomes the input of d axis decoupling controller. In Fig. 2(c), the q axis control signal i_{qsI}^* of the inverter is produced by pulsing i_{qL} with i_{qsM}^*. Similarly, the error signal of i_{qsI}^* includes i_{qsM}^*, where the q axis control signal v_q' can be designed according to the relationship of i_{qsM} and v_q' in Eq. (10), and becomes the input of q axis decoupling controller. Designing the d axis decoupling controller in Fig. 2(b) with Eq. (8), the input signals are v_d', i_{qsM} and ω_e, respectively and the output is v_d. Similarly, designing the q axis decoupling controller in Fig. 2(c) with Eq. (9), the input signals are v_q', i_{dsM}, ω_e and Ψ_{dr}, respectively and the output is v_q. After putting v_d and v_q into synchronous rotating dq axes to abc axes inverse transformation, the control signals V_a^*, V_b^* and V_c^* will be available to control the inverter output system voltages V_a, V_b and V_c.

III. FRAMEWORK OF SYSTEM

In this paper, the vector controller of inverter-excited induction generator design has a control core that is the DSP TMS320F240, which is a 16-bit chip with fix-point design and having not only the characteristic of a DSP but also enhanced

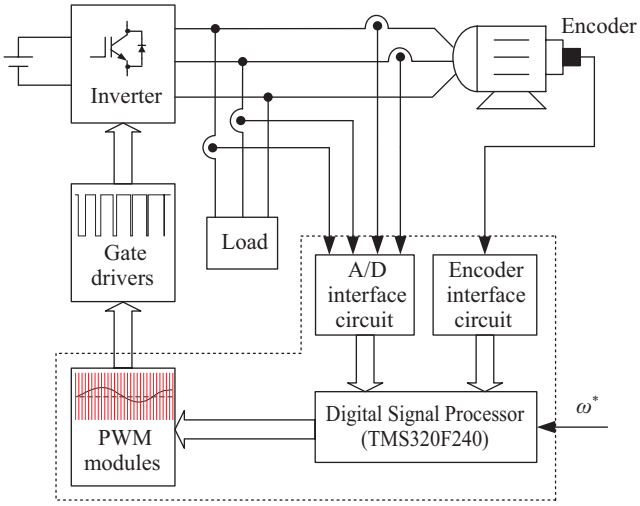

Fig. 3. The framework of system.

Harvard architecture, produced by TI company. And the program and data are processed in different buses so that the processing speed is greatly increased. The chip has very good advantage in reducing hardware circuit and also has convenience in program design. The framework of system is shown in Fig. 3.

In Fig. 3, the detection of rotor's position is done by the increase encoder, and then processed by the encoder interface of the digital signal module. The current detection device uses Hall current sensor to transform the three phase induction generator current i_{aM}, i_{bM} and i_{cM} and also three phase load current i_{aL}, i_{bL} and i_{cL} into voltage signals. And then the signals will be passed through the level adjustment circuit for satisfying the input voltage requirement of TMS320F240 A/D module, and proceeded by software program. Finally, using PWM, the three phase voltage commends (V_a^*, V_b^* and V_c^*) are generated for output. Here, we should point out that the hardware circuit outside the dashed line in Fig. 3 includes power transistor module, which can transform the voltage of battery into alternating electricity, and the gate driver circuit of transistor, so as to complete the vector control system of inverter-excited induction generator.

When the hardware framework is completed, software is needed to realize the vector control rule of the inverter-excited induction generator. In practice, this article uses assembly language to write the control rules derived by theory, and then the control is achieved by the encoder interface circuit built inside the DSP, current feedback, A/D interface and PWM module. The overall flow chart for realizing the vector control rule of the inverter-excited induction generator is shown in Fig. 4.

Remark: Here, with respect to Fig. 4, we should point out that the process of d and q axis control is excited at the same time for avoiding the phase lag. And the significant steps are expressed briefly as follows.

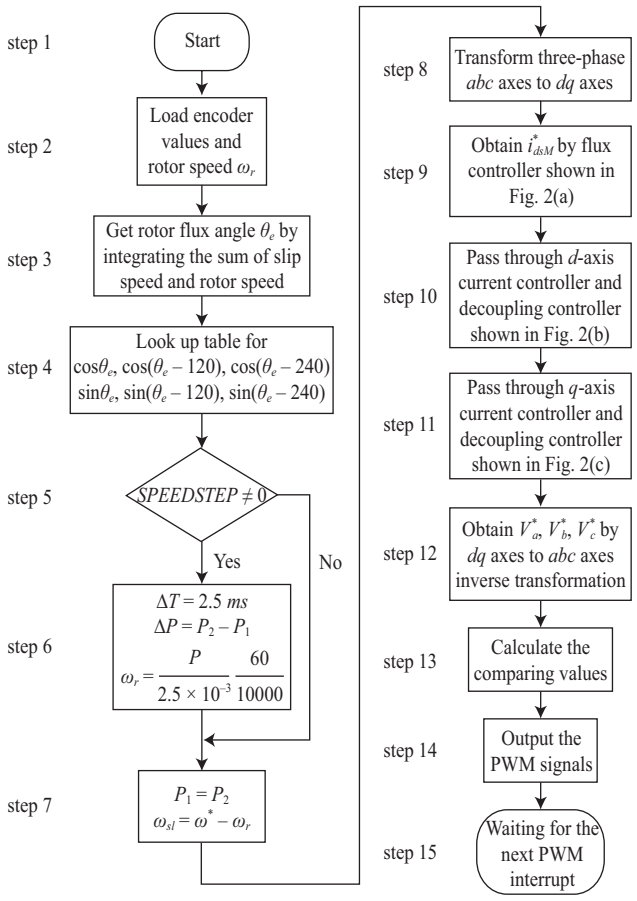

Fig. 4. Flow chart for realizing the vector control rule of the inverter-excited induction generator.

(i) In step 6, the calculation of rotor speed ω_r can be referred to Eq. (11).
(ii) In step 8, the transformation about three-phase abc axes to *dq* axes can be referred to [15, 16].
(iii) In step 9, by using the flux controller shown in Fig. 2(a), the i^*_{dsM} is obtained.
(iv) In step 12, by using the *dq* axes to *abc* axes inverse transformation, the control signals V_a^*, V_b^* and V_c^* are obtained [2, 6].

In Fig. 4, the program of rotor speed calculation by software is as follows. The pulse wave signal outputted by the encoder of the induction generator rotating shaft is transmitted to the encoder interface circuit of the DSP. The sampling time is 2.5 ms, and ΔP is calculated. Here, ΔP is the pulse wave number outputted by the encoder during the sampling time. In this paper, the encoder having 2500 pulse wave number per cycle is used. And then proceeding with fourfold circuit, the 10000 pulse wave numbers per cycle is obtained. Thus, the rotor speed ω_r can be calculated as following:

$$\omega_r = \frac{\Delta P}{2.5 \times 10^{-3}} \frac{60}{10000} \tag{11}$$

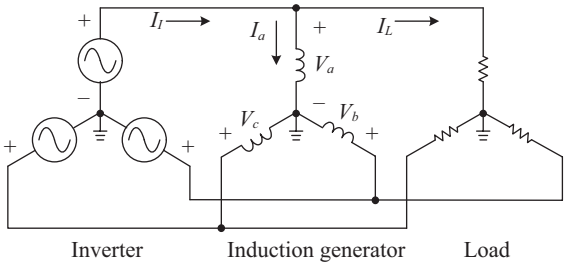

Fig. 5. The structure of system for experiment.

IV. EXPERIMENTAL RESULTS

In this section, using experiment, the proposed method will be verified and its performance also will be expressed. Now, the structure of system for experiment is shown in Fig. 5, in which the specification of the induction generator is three phases and 6 poles, 60 Hz, 220 V and 1 HP.

In Fig. 5, the measure points of induction generator are three phase voltages V_a, V_b and V_c, while the measure points of current are the *a*-phase output current I_I of the inverter, the *a*-phase output current I_a of the induction generator and the *a*-phase load current I_L, respectively. In Fig. 5, using power oscilloscope, the waveforms of V_a, V_b, V_c, I_I, I_a and I_L, which are operated at different modes, are recorded in Figs. 6-9. Here, we should point out that the Figs. 6-9(a) are experimental test waveforms (200 V/Div, 5 A/Div, 5 ms/Div), the Figs. 6-9(b) are vector diagrams according to Figs. 6-9(a), and the Figs. 6-9(c) are simulation waveforms (100 V/Div, 1.25 A/Div, 5 ms/Div) used the CASPOC software of simulation research.

For illustrating the experimental results conveniently, the relationship between *dq* axes vector and three phases *abc* axes is stated again about Fig. 5. In theory, the excited current of each phase of the induction generator is 90^o lagged behind voltage. If the phase current of the three phase induction generator is as following:

$$\begin{aligned} I_a &= I_m \sin \omega t \\ I_b &= I_m \sin(\omega t - 120^\circ) \\ I_c &= I_m \sin(\omega t + 120^\circ) \end{aligned} \tag{12}$$

Then the phase voltage is:

$$\begin{aligned} V_a &= V_m \cos \omega t \\ V_b &= V_m \cos(\omega t - 120^\circ) \\ V_c &= V_m \cos(\omega t + 120^\circ) \end{aligned} \tag{13}$$

Substitute Eqs. (12) and (13) to *dq* axes, then Eq. (14) will be obtained.

$$v_{qs} = V_m, v_{ds} = 0, i_{qs} = 0 \text{ and } i_{dsM} = I_m \tag{14}$$

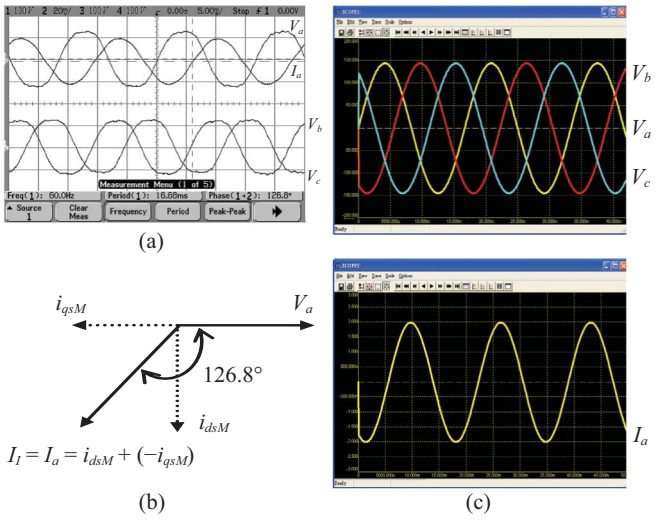

Fig. 6. Experimental results for induction generator without load (1300 rpm).

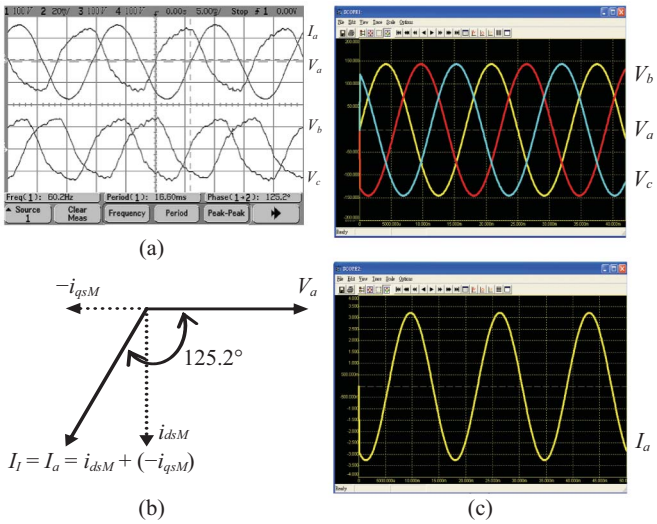

Fig. 7. Experimental results for induction generator without load (1400 rpm).

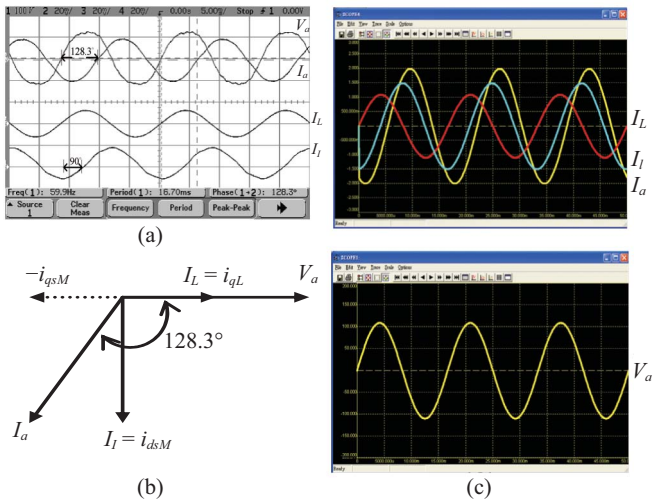

Fig. 8. Experimental results for induction generator with load (1300 rpm).

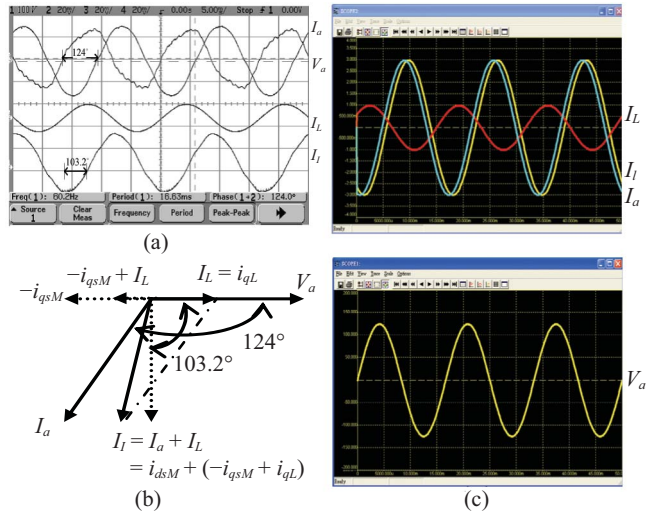

Fig. 9. Experimental results for induction generator with load (1400 rpm).

Compare Eq. (14) with Fig. 5, if the *a*-phase of the induction generator is aligned with *q* axis, then $v_{qs} = V_a$ and $i_{dsM} = I_a$.

In Fig. 6(a), the inverter provides excited current to the induction generator, and a DC motor simulates wind power to drive the induction generator to operate above synchronous. The load is with open loop in this experiment, thus the output current $-i_{qsM}$ of the induction generator will charge the battery by way of inverter. From Fig. 6(b), it is known that the output current of the inverter includes the excited current i_{dsM} and the output current $-i_{qsM}$ of the induction generator.

The rotating speed in Fig. 6(a) is 1300 rpm while in Fig. 7(a) is 1400 rpm. Comparing the results of Fig. 7(a) with Fig. 6(a), since the rotating speed is raised, then the theory predicts that the output current $-i_{qsM}$ of the induction generator increases as well as i_{dsM} and dq components will increase. Thus I_a is increased but the value changing of phase angle is not large. The experiment results are coincide with the theory predicts when rotating speed is increases.

In Fig. 8(a), the experiment conditions are the same with Fig. 6(a) but the difference is that the induction generator is connected to load. From Fig. 8(b) it is known that the inverter current I_I is 90° lagged behind the induction generator voltage V_a, the inverter only provides excited current i_{dsM} to the induction generator, and the output current $-i_{qsM}$ of the induction generator is equal to the load current I_L for the sake of the load is only resistance.

The load in Fig. 8(a) remains unchanged but raises the rotating speed to 1400 rpm, the experimental results will be obtained as in Fig. 9(a). Fig. 9(b) shows the vector diagram of the voltage and current waveform phase relation for Fig. 9(a).

Comparing the results of Fig. 9 with Fig. 8, the load of induction generator is the same but the rotating speed increases which means the induction generator outputs is more power and the output current $-i_{qsM}$ of the induction generator is larger than the load current, and the difference amount between each other will be absorbed by the inverter and will charge the battery. Thus, in Fig. 9(b), $I_I = I_a + I_L = -i_{qsM} + i_{qL} + i_{dsM}$. Since the inverter absorbs some current outputted from the induction generator, the current of inverter is lagged more than 90° behind the voltage. The actual value for experiment measurement is 103.2°, which means the experiment result is coincide with the theory predict.

V. CONCLUSION

In this paper, using the DSP as the core of system control, the vector controller of inverter-excited induction generator is designed. Also, a vector controller combining flux control and decoupling current control with respect to the VSCF system of the induction generator is proposed. From the experimental results, it is shown that the vector control approach applied in the induction generator can obtain a constant frequency output at different rotating speeds, and can overcome the difficulties of control for induction generator. Thus, the efficiency of the wind power generation system can be increased without using the mechanical speed regulator. Furthermore, from the small difference value between experiment result and theory predict, it has proved that the VSCF generating system on the induction generator can really control the output power of the induction generator under variable loading and different rotating speeds. In the future, we will develop this approach to high performance complex systems.

REFERENCES

1. Blaschke, F., "The principle of field orientation as applied to the new transvektor closed-loop control system for rotating-field machines," *Siemens Review*, Vol. 39, No. 5, pp. 217-220 (1972).
2. Bose, B. K., *Power Electronics and AC Drivers*, Prentice Hall, New Jersey (1986).
3. Brdys, M. A. and Malinowski, K., *Computer Aided Control System Design*, Word Scientific, pp. 425-447 (1996).
4. Cardenas, R. and Pena, R., "Sensorless vector control of induction generators for variable-speed wind energy applications," *IEEE Transactions on Energy Conversion*, Vol. 19, No. 1, pp. 196-205 (2004).
5. Geholt, N. S. and Alsina, P. J., "Deadbeat controlled field oriented induction motor with reduced order rotor flux observer," *IECON-1991*, Kobe, Japan, pp. 573-578 (1991).
6. Incze, A. M., Szabo, I. I., and Imecs, M. C., "Vector control schemes for tandem-converter fed induction motor drives," *IEEE Transactions on Power Electronics*, Vol. 20, No. 2, pp. 493-501 (2005).
7. Krause, P. C., *Analysis of Electric Machinery*, McGRAW-Hill, Inc. (1987).
8. Lin, C. H., "Impact of fire-through and misfire in rectifier valves on a turbine generator neighboring to a HVDC inverter station," *Journal of Marine Science and Technology*, Vol. 16, No. 4, pp. 241-249 (2008).
9. Lu, F. S., Tseng, C. H., and Wu, B. C., "Design and implementation of an all-digital real-time underwater acoustic transceiver using digital signal processors," *Journal of Marine Science and Technology*, Vol. 16, No. 1, pp. 34-43 (2008).
10. Mathew, S., Pandey, K. P., and Kumar, V., "Analysis of wind regimes for energy estimation," *Renewable Energy*, Vol. 25, pp. 381-399 (2002).
11. Oh, D. S., Cho, K. Y., and Youn, M. J., "New rotor parameter estimation for a flux and speed control of induction generator considering saturation effects," *IECON-1991*, Kobe, Japan, pp. 561-566 (1991).
12. Shiao, Y. S. and Lin, C. E., "A prototype induction generator VSCF system for aircraft," *International IEEE/IAC conference on Industrial Automation and Control*, Taipei, Taiwan, pp. 148-155 (1995).
13. Slootweg, J. G., Haan, S. W. H., Polinder, H., and Kling, W. L., "General model for representing variable speed wind turbines in power system dynamics simulations," *IEEE Transactions on Power System*, Vol. 18, No. 1, pp. 144-151 (2003).
14. Stephan, R. M., "Field oriented and field acceleration control for induction motors," *IECON-1991*, Kobe, Japan, pp. 567-572 (1991).
15. Studtmann, G. H., "Application of power electronic switching techniques to induction generators," *IEEE Industry Applications System Conference Proceding*, pp. 474-481 (1984).
16. Tzou, Y. Y., "DSP-based robust control of an AC induction servo drive for motion control," *IEEE Transactions on Control System Technology*, Vol. 4, No. 6, pp. 614-626 (1996).
17. Wang, L. and Yeh, T. H., "Model establishment and simulation analyses of wind power generation systems," *The 25th Symposium on Electrical Power Engineering*, Taipei, Taiwan, pp. 29-36 (2004).
18. Wekhande, S. and Agarwal, V., "Simple control for a wind-driven induction generator," *IEEE Industry Applications Magazine*, Vol. 7, No. 2, pp. 44-53 (2001).